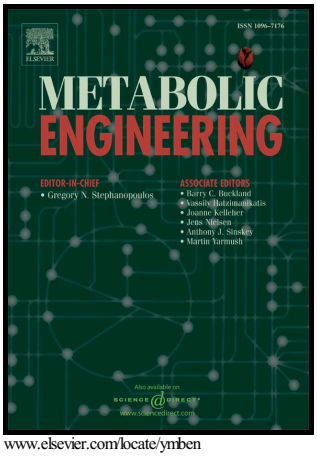

www.elsevier.com/locate/ymben

Towards acetone-uncoupled biofuels production in solventogenic *Clostridium* through reducing power conservation

Dong Liu, Zhengjiao Yang, Ping Wang, Huanqing Niu, Wei Zhuang, Yong Chen, Jinglan Wu, Chenjie Zhu, Hanjie Ying, Pingkai Ouyang

PII: S1096-7176(17)30353-1
DOI: https://doi.org/10.1016/j.ymben.2018.03.012
Reference: YMBEN1366

To appear in: *Metabolic Engineering*

Received date: 13 September 2017
Revised date: 11 March 2018
Accepted date: 11 March 2018

Cite this article as: Dong Liu, Zhengjiao Yang, Ping Wang, Huanqing Niu, Wei Zhuang, Yong Chen, Jinglan Wu, Chenjie Zhu, Hanjie Ying and Pingkai Ouyang, Towards acetone-uncoupled biofuels production in solventogenic *Clostridium* through reducing power conservation, *Metabolic Engineering,* https://doi.org/10.1016/j.ymben.2018.03.012

Towards acetone-uncoupled biofuels production in solventogenic *Clostridium* through reducing power conservation

Dong Liu,[a,b] Zhengjiao Yang,[a] Ping Wang[c], Huanqing Niu,[a,b] Wei Zhuang,[a,b] Yong Chen,[a,b] Jinglan Wu,[a,b] Chenjie Zhu,[a,b] Hanjie Ying[a,b,*] and Pingkai Ouyang[a,b]

[a]State Key Laboratory of Materials-Oriented Chemical Engineering, College of Biotechnology and Pharmaceutical Engineering, Nanjing Tech University, No. 30, Puzhu South Road, Nanjing 211816, China.

[b]Jiangsu National Synergetic Innovation Center for Advance Material (SICAM), No. 30, Puzhu South Road, Nanjing 211816, China.

[c]State Key Laboratory of Bioreactor Engineering, Biomedical Nanotechnology Center, East China University of Science and Technology, Shanghai 200237, P.R. China.

[*]Corresponding author. Tel: +86 25 58139992; Fax: +86 25 58139389.

yinghanjie@njtech.edu.cn

Abstract

Microbial production of butanol by solventogenic *Clostridium* has long been complicated with the formation of acetone as an unwanted product, which causes poor product yields and creates a most important problem concerning substrate transformation. Intensive attempts concentrate on carbon conversion pathways to eliminate acetone, but have actually achieved little so far. Here, we believe microbial product distribution can largely depend on how the cell plays its energetic cofactors in central metabolism, and demonstrate that by introducing a synthetic 2,3-butanediol

synthesis pathway in *Clostridium acetobutylicum* as an NADH-compensating module to readjust the reducing power at a systems level, the production of acetone can be selectively and efficiently eliminated (<0.3 g/L). H_2 evolution was reduced by 78%, and the total alcohol yield was strikingly increased by 19% to 0.44 g/g glucose, much higher than those yet reported for butanol fermentation. These findings highlight that it is the loss of reducing power rather than typically manipulated solventogenesis genes that dominates acetone formation. Further study revealed that the NADH-module triggered apparent regulation of pathways involved in electron transfer and reducing power conservation. The study also suggested the key to conservation of intracellular reducing power might essentially lie in the intermediate processes in central metabolism that are related to redox partners, butyrate or C_4 branches, and possibly NADH and NADPH specificity. This study represents the first effective redox-based configuration of *C. acetobutylicum* and provides valuable understandings for redox engineering of native *Clostridium* species towards advanced production of biofuels and alcohols.

Keywords: redox cofactor, NADH, atom economy, biobutanol, *Clostridium acetobutylicum*, 2,3-butanediol

1. Introduction

Solventogenic *Clostridium* species are capable of biosynthesizing a range of liquid fuels and alcohols such as isopropanol, butanol, ethanol and 2,3-butanediol, which is of particular importance for energy and environmental issues. One canonical example

is the Acetone-Butanol-Ethanol (ABE) fermentation by *Clostridium acetobutylicum*, which represents one of the oldest and once best-established worldwide industries (Green, 2011; Jones and Woods, 1986). Historically, ABE fermentation was recruited to produce acetone for preparation of ammunitions. Today, however, this process is extensively explored to produce biofuel butanol. Consequently, acetone formation becomes unfavourable and a major limitation on the viability of biobutanol (Jiang et al., 2014; Tracy, 2012). Acetone is produced by decarboxylation of glucose with evolution of considerable CO_2 and hydrogen, thus causing poor atom economies as well as low product prices.

Intensive attempts have been made to eliminate acetone formation by manipulating the solventogenesis pathway genes, but acetone could not be effectively abolished without causing significant undesired effects. Disruption of the acetone-forming gene either *adc* or *ctfAB* could abolish acetone, but led to accumulation of an equivalent amount of acetate and butyrate (actually the precursor of acetone) as well as reduced butanol titers (Croux et al., 2016; Jiang et al., 2009). Studies employing antisense RNA against acetone-forming genes failed to achieve adequate results, either (Tummala et al., 2003a; Tummala et al., 2003b). Since acetone is formed in reactions that are coupled to the re-assimilation of acetate and butyrate (Hartmanis et al., 1984), studies were also carried out to disrupt the acetate-forming genes *ack* and *pta*, or the butyrate-forming genes *buk* and *ptb*, or both the acid- and acetone-forming genes. Still, the production of acetone and acids could not be effectively eliminated and/or no significant improvement in alcohol production was observed (Jang et al., 2012; Kuit

et al., 2012; Lütke-Eversloh and Bahl, 2011; Lehmann et al., 2012). Jang et al. conducted a systematic study of the solventogenesis genes and by disruption of particular acids forming genes with simultaneous overexpression of an optimized alcohol dehydrogenase, butanol yield was improved to 0.31 g/g glucose, which can be considered as the best result ever obtained by manipulation of solventogenesis genes in *C. acetobutylicum* (Jang et al., 2012). However, consistent with earlier studies, acetone was not fully eliminated and the total solvent yield was decreased. Altogether, these results indicate that manipulation of solventogenesis pathway genes to eliminate acetone seems not as effective as is expected.

Some physiological roles have been proposed to explain the intrinsic formation of acetone in *C. acetobutylicum* (Desai et al., 1999a; Hartmanis et al., 1984). However, acetone can be considered as an oxidation product from glucose, and its formation may be associated with the redox power in the cells. In view of redox balance, glucose could theoretically 100% (mol/mol) be converted to butanol with no acetone and H_2 formation (without considering cell growth). Nevertheless, the fact is that in *C. acetobutylicum* large amounts of reducing power are lost in H_2 form with simultaneous production of considerable amounts of acetone (Liu et al., 2013). Early studies showed that exogenous supplement of electron carriers such as methyl viologen (MV) (Grupe and Gottschalk, 1992; Rao and Mutharasan, 1986) or chemostat culture on substrates with high degree of reduction like glycerol (Girbal and Soucaille, 1994; Vasconcelos et al., 1994) could apparently reinforce the supply of reducing power and reduce acetone formation. To conserve the intracellular

reducing power in *C. acetobutylicum*, inactivation of the hydrogenase was performed by several groups, but no mutant could be obtained despite repeated attempts (Cooksley et al., 2012; Liu et al., 2015). Although disruption of the hydrogenase gene was recently reported successful in a *C. acetobutylicum* strain, it showed little impact on the product pattern (Jang et al., 2014). Usually, formate dehydrogenase (FDH) can be used to generate NADH by using formic acid as a substrate. However, it was showed that expression of FDH gene in *C. acetobutylicum* did not affect intracellular NADH/NAD+ level (Wang et al., 2011). So far, no genetic constructs are able to effectively reinforce the supply of reducing power in *C. acetobutylicum*. How to effectively configure *C. acetobutylicum* to enhance its reducing power conservation and to what extent this will impact acetone formation remains to be investigated.

In this study, we speculate the involvement of reducing power in acetone formation, and propose an NADH-compensation strategy in *C. acetobutylicum* for the first time based on 2,3-butanediol biosynthesis. Biosynthesis of 2,3-butanediol from glucose generates reducing power NADH. In typical acetoin and 2,3-butanediol producing strains, the redundant NADH was consumed under aerobic conditions or even directly oxidized into H_2O by introduction of NADH oxidase (Bae et al., 2016; Kim et al., 2015). In anaerobic *C. acetobutylicum*, the NADH generated from 2,3-butanediol synthesis should compensate for the deficiency of reducing power (Figure 1). Although no NADH is directly involved in acetone branch, and 2,3-butanediol biosynthesis also seems to have nothing to do with the acetone pathway, we are going to demonstrate herein that introduction of such an NADH-generating 2,3-butanediol

pathway enables selective and effective elimination of acetone at a systems level, without manipulating any of the solventogenesis genes and without causing significant undesired effects.

2. Materials and methods

2.1 Plasmids, bacterial strains and growth conditions

The plasmids and bacterial strains used in this study are listed in Table1. *Escherichia coli* strains were grown at 37 °C in LB medium supplemented with appropriate antibiotics (100 μg/mL ampicillin and/or 25 μg/mL tetracycline according experimental design). *C. acetobutylicum* strains were grown in P2 medium (Baer et al., 1987) containing 10 g/L glucose as the sole carbohydrate source, supplemented with an antibiotic (10 ug/mL erythromycin or 15 ug/mL thiamphenicol) as required at 37 °C in an anaerobic chamber (Bug Box, Ruskinn Technology, Leeds, UK).

2.2 Gene disruption

The generation of *C. acetobutylicum* mutants was performed using the ClosTron system based on a bacterial group II intron, as previously described (Heap et al., 2010). Briefly, sites and intron targeting regions (344-bp DNA fragments) for insertion into targeted genes were designed using a computer algorithm available at the ClosTron website (http://www.clostron.com/). The 344-bp DNA fragments were synthesized in Genewiz (Suzhou, China) and ligated into HindIII and BsrGI linearized pMTL007C-E2 plasmids. Detailed DNA sequences are listed in Supplementary File 1:

Table S1. Before electroporation, the plasmids were methylated in *E. coli* Top10 (pAN2) to avoid the natural restriction system of *C. acetobutylicum* (Mermelstein and Papoutsakis, 1993). The plasmids were then transformed into *C. acetobutylicum* as described previously (Mermelstein et al., 1992) and selected on P2 agar containing thiamphenicol. Colonies were re-streaked on plates containing erythromycin to select integrants. The insertions were validated by PCR screening and sequencing of the insertion area using the respective primers listed in Table S1. Loss of the pMTL007C-E2 backbone by the mutants during successive transfers on thiamphenicol-free plates was also confirmed.

2.3 Gene expression

Genes for overexpression were synthesized (Genewiz, Suzhou, China) or amplified by PCR from bacterial genomic DNA using the respective primers listed in Supplementary File 1: Table S1, followed by ligation to NdeI-linearized pSY8 plasmids based on homologous recombination using the one-step clone kit (Vazyme Biotech Inc., Nanjing, China). For multi-gene expression, genes were assembled in the *alsD-budh-alsS* order according their contribution to 2,3-butanediol production, and a ribosome binding site (RBS, 5'-AGGAGGTTAGTTAGA-3') was also added upstream of the translation initiation codon of the *budh* and *alsS* genes by PCR with primers containing the RBS sequence (Supplementary File 1: Table S1). These constructs placed the genes under the control of the phosphotransbutyrylase gene (ptb) promoter, which acts as a constitutive promoter in both *E. coli* and *C. acetobutylicum*

(Wardwell et al., 2001). The plasmids were methylated in *E. coli* Top10 (pAN2) and then electroporated into *C. acetobutylicum*. Cells were plated on P2 agar containing 15 μg/mL thiamphenicol and incubated at 37 °C for 24 h to select positive transformants that were further confirmed by PCR. Similarly, the empty vector pSY8 was also transformed into *C. acetobutylicum* B3, yielding a plasmid-control strain.

2.4 Fermentation and analysis

C. acetobutylicum fermentations were performed in P2 medium (glucose, 60 g/L; K2HPO4, 0.5 g/L; KH2PO4, 0.5 g/L; CH3COONH4, 2.2 g/L; MgSO4•7H2O, 0.2 g/L; MnSO4•H2O, 0.01 g/L; NaCl, 0.01 g/L; FeSO4•7H2O, 0.01 g/L; p-aminobenzoic acid, 1 mg/L; thiamine, 1 mg/L; biotin, 0.01 mg/L) at 37 °C. Experiments were conducted in 500-mL static Duran bottles with 300 mL of working volume at 37 °C. Each bottle was inoculated with 30 mL of 12-h–old seed culture and the OD_{600nm} of the initial culture was around 0.21. The cell density (OD_{600nm}), concentrations of residual sugars and metabolites (acids and solvents), were determined according to the methods described previously (Liu et al., 2013). Experiments were performed in triplicate and the mean value (± SD) was calculated.

2.5 Determination of metabolic flux change

$$2r_{Acoi} + 2r_{Ac} + r_{2,3\text{-}BD} + 2r_{But} + 4r_{Acon} - 0.873r_{Biomass} = r_{H2} \quad \text{Eq. (1)}$$

$$r_{Lac} + 2r_{Acoi} + r_{EtOH} + r_{Ac} + 2r_{2,3\text{-}BD} + 2r_{But} + 2r_{Acon} + 2r_{BuOH} + 2r_{Biomass} = -2r_{Glu} \quad \text{Eq. (2)}$$

The fluxes of glucose (r_{Glu}), acetoin (r_{Acoi}), acetone (r_{Acon}), lactate (r_{Lac}), acetate

(r_{Ac}), butyrate (r_{But}), ethanol (r_{EtOH}), butanol (r_{BuOH}) and 2,3-butanediol ($r_{2,3\text{-}BD}$) were determined experimentally by measuring their accumulation or consumption at the end of fermentation. The fluxes of biomass ($r_{Biomass}$) and H_2 (r_{H2}) were calculated with Eq. (1) and Eq. (2) previously deduced from the stoichiometry of *C. acetobutylicum* metabolism (Desai et al., 1999b; Liu et al., 2013). CO_2 evolution flux could also be calculated approximately from the product fluxes. In this way, the molar flux distributions in the wild strain and engineered DH2 strain were determined as Eq. (3) and Eq. (4), respectively:

$$100\times Glu = 1.6\times But + 29\times Acon + 5.9\times Acoi + 50\times BuOH + 15\times EtOH + 0.9 \times Lac + 8.6\times Biomass - 5.7\times Ac + 109\times H_2 + 210\times CO_2 \quad \text{Eq. (3)}$$

$$100\times Glu = 0.4\times But + 1.7\times Acon + 28\times 2,3\text{-}BD + 56\times BuOH + 24\times EtOH + 1.1 \times Lac + 3.6\times Biomass - 4.4\times Ac + 24\times H_2 + 194\times CO_2 \quad \text{Eq. (4)}$$

Thus, the metabolic flux change from the wild strain to the DH2 strain was interpreted as Eq. (5) then mathematically transformed into Eq. (6) which is approximately equal to Eq. (7):

$$1.6\times But + 29\times Acon + 5.9\times Acoi + 50\times BuOH + 15\times EtOH + 0.9 \times Lac + 8.6\times Biomass - 5.7\times Ac + 109\times H_2 + 210\times CO_2 = 0.4\times But + 1.7\times Acon + 28\times 2,3\text{-}BD + 56\times BuOH + 24\times EtOH + 1.1 \times Lac + 3.6\times Biomass - 4.4\times Ac + 24\times H_2 + 194\times CO_2 \quad \text{Eq. (5)}$$

$$0.04\times But + Acon + 0.22\times Acoi + 0.18\times Biomass + 3.2\times H_2 + 0.6\times CO_2 = 2,3\text{-}BD + 0.22\times BuOH + 0.34\times EtOH + 0.007 \times Lac + 0.05\times Ac \quad \text{Eq. (6)}$$

$$Acon + 0.22\times Acoi + 0.18\times Biomass + 0.6\times CO_2 + 3.2\times H_2 = 2,3\text{-}BD + 0.22\times BuOH$$

+ 0.34×EtOH Eq. (7)

2.6 Label-free proteome analysis

Cells were harvested at acidogenic phase (12 h for both wild B3 strain and DH2) and solventogenic phase (48 h for B3 strain and 60 h for DH2 strain, based on a similar metabolic stage) by centrifugation at 5000 g for 10 min and washed twice with PBS. Cells were resuspended in lysis buffer A (8 mol/L urea, 2 mol/L thiourea, 0.1% SDS and 1 mmol/L PMSF in 0.1 mol/L Tris-HCl buffer, pH8.5) and broken by sonication. Cell lysates were centrifuged at 10,000 g at 4 °C for 20 min, and the supernatants were precipitated by 5-fold volume cold acetone overnight at -20 °C. The precipitated pellets were resupended in lysis buffer B (8 mol/L urea, 2 mol/L thiourea in 0.1mol/L Tris-HCl buffer, pH 8.5), and concentration of total protein was determined by Bradford assay. Proteins (100 μg for each culture condition) were reduced, alkylated, digested, and cleaned up as previously reported (Shen et al., 2016). The resulting peptides were lyophilized.

LC-MS/MS analysis was performed on a Nano Aquity UPLC system (Waters Corporation, Milford, MA) connected to a Quadrupole-Orbitrap mass spectrometer (Q-Exactives) (Thermo Fisher Scientific, Bremen, Germany) equipped with an online nano-electrospray ion source. The lyophilized peptides were dissolved in 30 μL of solvent C (C: water with 0.1% formic acid), separated by nanoLC and analyzed by on-line electrospray tandem mass spectrometry. Five-μLpeptide sample was loaded onto the trap column (Thermo Scientific Acclaim PepMap C18, 100μm × 2cm), with a

flow of 10μL/min for 3 min and subsequently separated on the analytical column (Acclaim PepMap C18, 75μm × 15cm) with a linear gradient, from 2% D to 40% D (D: acetonitrile with 0.1% formic acid) in 100 min. The column was re-equilibrated at initial conditions for 15 min. The column flow rate was maintained at 300nL/min and column temperature was maintained at 40℃. The electrospray voltage was 1.9 kV.

All MS/MS data were processed with PEAKS Studio 8.0 (Bioinformatics Solutions Inc., Waterloo, ON, Canada) for searching against the UniProt *Clostridium acetobutylicum* proteome database containing 3853 entries. Default settings were used for search parameters: specific digestion with Trysin/P with up to two missed cleavages. Protein N terminal acetylation and methionine oxidation were set as variable modification, while cysteine alkylation was set as fixed modification. Parent mass error tolerance was set as 7.0 ppm and fragment mass error tolerance was set as 0.05 Da. Protein intensities were determined with PEAKS Q. The intensity for an individual protein is the average of triplicate samples. A fold change in protein intensity ≥ 2 ($P < 0.05$ by t-test) was considered significant.

2.7 Combined analysis of molecular basis from different studies

The transcriptomic data from Hönicke et al., 2012 and Yoo et al., 2017, and the proteomic data from Yoo et al., 2015 and this study, were used for a combined molecular basis analysis concerning *C. acetobutylicum* central metabolism. For all the data, only a gene or a protein with a ≥ 2-fold change was considered regulated. *C. acetobutylicum* produces solvents through solventogenesis and these data shared

genes/proteins regulation during a common solventogenic phase. Hence, only the genes/proteins regulated during the solventogenic phase were included and compared with a Venn diagram. For simplicity, proteins were presented as their encoding genes in the Venn diagram.

3. Results

3.1 Identification of the key gene for acetoin production

To construct the NADH-generating 2,3-butanediol biosynthesis module, *C. acetobutylicum* was first engineered to improve production of precursor acetoin before 2,3-butanediol dehydrogenases were further introduced. Biosynthesis of acetoin requires *alsS* (α-acetolactate synthase gene), *alsD (*α-acetolactate decarboxylase gene), and typically a transcription factor gene *alsR*. *C. acetobutylicum* has these genes, but unlike in many other species, these genes are not situated in an operon and they are not well studied. Thus, the specific impacts of these genes in *C. acetobutylicum* were first investigated (Table 2). Results showed that, although *aslR* is required in many acetoin-producing species, this gene had no essential role in acetoin production in *C. acetobutylicum*, as the product pattern was not significantly altered when *alsR* was either disrupted or overexpressed. As for the *alsS* gene, overexpression of this gene slightly increased acetoin production, but it significantly reduced butanol production as well (Table 2). Meanwhile, obvious growth retardation was found for both *C. acetobutylicum* and *E. coli* harboring the *alsS*-overexpressing plasmid. This toxic effect of *alsS* overexpression had also been reported in some other species

(Higashide et al., 2011; Li and Liao, 2014; Li et al., 2014b). Among these genes only the *alsD* showed a great contribution to acetoin production. Overexpression of the *alsD* dramatically improved acetoin from 1.6 to 5.0 g/L. Thus, *alsD* was the key gene for acetoin production and was selected for subsequent construction of the NADH-compensating module.

3.2 Expression of heterologous *alsD* genes

Different *alsD* genes from well-known acetoin-producing species including three G+ strains, *B. subtilis* 168 (Xiao and Lu, 2014), *Bacillus licheniformis* ATCC14580 (Oliver et al., 2013), and *Paenibacillus polymyxa* DSM365 (Xie et al., 2015), and three G- strains, *Enterobacter cloacae* SDM (Xu et al., 2012), *Klebsiella pneumoniae* KCTC2242 (Lee et al., 2012), and *Serratia marcescens* ATCC14041 (Li et al., 2014a) , were investigated (Table 2). Although all these genes encode α-acetolactate decarboxylases with comparable lengths (249-260 aa), they showed interesting differences when expressed in *C. acetobutylicum*. Generally, expression of these genes could all increase acetoin production and decrease acetone formation. However, the *alsD* genes from G+ strains seemed to decrease acetone to a more extent than those from the G- strains. The best performance was obtained by expression of the $alsD_{bsu}$ gene from *B. subtilis*. Expression of the $alsD_{bsu}$ gene increased acetoin production by 281% to 6.1 g/L and reduced acetone production by 61% to 1.9 g/L with a significantly improved solvent yield (Table 2), a performance even better than that obtained with the *alsD* gene from *C. actobutylicum* itself. Thus, the $alsD_{bsu}$ gene

was used for construction of the NADH-compensating module.

3.3 Introduction of 2,3-butanediol dehydrogenases

Different 2,3-butanediol dehydrogenase genes, the *bdhA* from *B. subtilis* 168 (Yan et al., 2009), the *acr* (*C_bei1464*) from *C. beijerinckii* NCIMB 8052 (Siemerink et al., 2011), the *bdh* (*CAETHG_0385*) from *Clostridium autoethanogenum*n JAI-1 (Köpke et al., 2014), and the *budC* from *K. pneumoniae* MGH78578 (Yan et al., 2009), were individually introduced into *C. acetobutylicum*. Expression of these genes could effectively produce 2,3-butanediol from acetoin (Table 3). However, the 2,3-butanediol titer produced by each of these 2,3-butanediol dehydrogenase genes alone was generally comparable to the acetoin titer natively produced in wild *C. acetobutylicum*. This suggested that acetoin biosynthesis was roughly rigid in wild *C. acetobutylicum* and biosynthesis of 2,3-butanediol was limited by acetoin availability. Therefore, the 2,3-butanediol dehydrogenase gene (only $bdhA_{bsu}$ and acr_{cbe} were demonstrated at this point) was co-expressed with the $alsD_{bsu}$ gene that had showed the greatest contribution to acetoin production. Compared to expression of 2,3-butanediol dehydrogenase gene alone, co-expression of $alsD_{bsu}$ with 2,3-butanediol dehydrogenase gene greatly increased 2,3-butanediol production and reduced acetone formation (Table 3). To increase the translation efficiencies for 2,3-butanediol dehydrogenases, a RBS sequence (AGGAGGTTAGTTAGA) from the *thlA* gene in *C. acetobutylicum* was introduced upstream of the 2,3-butanediol dehydrogenase genes in the expression cassettes (Figure 2). This further increased

2,3-butanediol production. In particular, the 2,3-butanediol produced by the strain co-expressing *bdhA*$_{bsu}$ with *alsD*$_{bsu}$ was dramatically increased to 7.9 g/L upon introduction of the RBS.

Here, expression of *alsS* genes was tried again by locating them behind *alsD*$_{bsu}$ and *bdhA*$_{bsu}$, hoping to moderately attenuate their expression. However, their toxicity effects still could not be overcome.

3.4 Co-expression of complementary 2,3-butanediol dehydrogenase isozymes

Although a high 2,3-butanediol titer was produced by the *alsD*$_{bsu}$-RBS-*bdhA*$_{bsu}$ construct, a small amount of acetone and acetoin remained. The residual acetoin and acetone would create a dilemma for product recovery. After examining the detailed performances of the 2,3-butanediol dehydrogenase genes, it was found that the 2,3-butanediol dehydrogenase isozymes displayed distinct catalytic properties (See Table 3, and also summarized in Supplementary File 1: Table S2). The enzyme from *B. subtilis* (*bdhA*$_{bsu}$) yielded relatively high 2,3-butanediol titers but incomplete acetoin conversion, suggesting this enzyme might have a high activity but a low affinity. On the Other hand, the enzyme from *C. beijerinckii* (*acr*$_{cbe}$) yielded complete acetoin conversion but relatively low 2,3-butanediol titers, suggesting this enzyme might have a high affinity but low activity. So, these two isozymes of 2,3-butanediol dehydrogenase seemed complementary in terms of catalytic properties and were thus expressed together (*alsD*$_{bsu}$-RBS-*bdhA*$_{bsu}$-RBS-*acr*$_{cbe}$). The result showed that acetoin could be completely converted and at the same time a relatively high 2,3-butanediol

titer was obtained, a performance combining the advantages of both isozymes (Table 3). Strikingly, acetone was completely eliminated to a negligible level (<0.3 g/L). The solvent yield of the final strain, designated DH2, was dramatically improved to 0.439 g/g glucose, the highest solvent yield yet reported for ABE fermentation.

3.5 Redirection of metabolic fluxes

C_3H_6O (acetone) + 0.22×$C_4H_8O_2$ (acetoin) + 0.18×Biomass + 0.6×CO_2 + 3.2×H_2 = $C_4H_{10}O_2$ (butanediol) + 0.22×$C_4H_{10}O$ (butanol) + 0.34×C_2H_6O (ethanol) Eq. (7)

C_3H_6O (acetone) + CO_2 + 3×H_2 = $C_4H_{10}O_2$ (butanediol) + H_2O Eq. (8)

With the introduction of the NADH-compensating 2,3-butanediol pathway in *C. acetobutylicum*, the metabolic flux towards acetone in DH2 strain was reduced by 94%, creating a "reaction" transforming acetone into 2,3-butanediol. Provided with reducing power, the transformation of acetone into 2,3-butanediol can be virtually as Eq. (8). The actual metabolic flux change (deduced in section 2.5, Figure 3) was approximately as Eq. (7). The stoichiometric coefficients of Eq. (7) are adequately close to those of Eq. (8), except the coefficient of CO_2 whose deviation can be explained by the involvement of background acetoin and change in biomass. The similarity between Eq. (7) and Eq. (8) suggests that the elimination of acetone in DH2 strain was indeed attributed to enhanced reducing power. Obviously, the transformation of low-molecular-weight oxidation product acetone (Mr = 58) into 2,3-butanediol (Mr = 90) was accomplished by decreasing hydrogen and CO_2 production, which could significantly increase the atom economy. Indeed, compared

to the wild strain, the H_2 flux in DH2 strain was reduced by 78% (Figure 3), and CO_2 was calculated to be reduced by 8%, accounting for the improved product yield in DH2.

Importantly, the NADH-compensating module apparently reversed the loss of electron at the pyruvate node. According to the metabolic fluxes in Figure 3, 49% of the reduced ferredoxin (FdH_2) formed in a reaction coupled to pyruvate decarboxylation as well as in a reaction coupled to crotonyl-CoA reduction were lost as H_2 in the wild strain, whereas only 12% was lost in the DH2 strain. So, not only did the 2,3-butanediol biosynthesis module serve to generate extra reducing power, it also triggered conservation of intracellular reducing power, which is of particular implications that are discussed below.

3.6 Proteomic responses of *C. acetobutylicum* to the NADH-compensation

Proteomic analysis (Supplementary File 2) showed that while glycolysis, pentose phosphate pathways and TCA cycle were basically unaffected in the DH2 strain, pyruvate catabolism and solvent production among the central metabolism were particularly regulated, and most of the regulated proteins are involved in electron (or hydrogen) transfer and conservation (Table 4 and Figure 4). The elimination of acetone in the DH2 strain was also supported by 3- to 5-fold lower expression of Adc and 30- to 1000-fold lower expression of CtfAB. For alcohol production, the NADH-dependent aldehyde dehydrogenase AdhE1 and the NADPH-dependent butanol dehydrogenase BdhB that are typically predominantly used by *C.*

acetobutylicum to produce butanol (Yoo et al., 2015), were down-regulated 30- to 50-fold and 2.5- to 5-fold, respectively. Two other alcohol dehydrogenases, the NADPH-dependent butanol dehydrogenase BdhC and an uncharacterized CA_P0059 were down-regulated 2- to 3-fold as well. On the other hand, the bifunctional NADH-dependent aldehyde-alcohol dehydrogenase AdhE2, was observed up-regulated 3- to 21-fold instead. This was consistent with previous findings that AdhE2 was antagonistically regulated to AdhE1 and specifically recruited for alcohol production with diminished acetone formation (Hönicke et al., 2012; Yoo et al., 2015). The pyruvate-ferredoxin/flavodoxin oxidoreductase (CA_C2229) that dominates the conversion of pyruvate to acetyl-CoA in *C. acetobutylicum* and proteins that probably serve as alternative enzymes to catabolize pyruvate were all apparently down-regulated. This might be attributed to reduced pyruvate stress due to the channelling of pyruvate towards 2,3-butanediol. A ferredoxin (CA_C0303), the key redox partner of the major hydrogenase HydA in *C. acetobutylicum*, was down-regulated 2.5-fold while a flavodoxin (CA_C3486) was up-regulated 3- to 7-fold. Flavodoxin could replace ferredoxin as an electron carrier in many reactions, and down-regulation of CA_C0303 and/or up-regulation CA_C3846 was also observed under other enhanced reducing power conditions (Hönicke et al., 2012; Yoo et al., 2015; Yoo et al., 2017). The most up-regulated proteins of central metabolism were an electron transfer flavoprotein (Etf, α, β subunits) dependent dehydrogenase complex EtfAB-Fcd (11- to 44-fold). *C. acetobutylicum* has two EtfAB-dependent dehydrogenase complexes: one is the EtfAB-Fcd encoded by CA_C2542-2544 and

the other one is the butyryl-CoA dehydrogenase complex EtfAB-Bcd encoded by CA_C2709-2711. Compared to the well characterized EtfAB-Bcd, EtfAB-Fcd has been rarely reported. So far, only one study have shown that the *etfAB-fcd* cluster could affect carbon flux flowing through the C_4 pathways, and disruption of the *fcd* gene led to particular accumulation of butyrate (Xu, 2014). Therefore, EtfAB-Fcd is probably relevant to butyrate flux and its dramatic up-regulation might account for the diminished butyrate formation in DH2 strain.

Besides central metabolism, amino acid metabolism was apparently affected in the DH2 strain. A 3- to 10-fold down-regulation of proteins involved in biosynthesis of arginine (ArgB-D, ArgJ and ArgF-H), histidine (HisA-I and HisZ), tryptophan (PabA, ParB, TrpA-D and TrpF), and sulfate uptake (CA_C0106-10108, CysD and CysN) and incorporation to produce cysteine (CA_C0102) and methionine (MetH) were observed. By contrast, proteins involved in biosynthesis of branched-chain amino acids (LeuB-D, IlvB and IlvD) were up-regulated 9- to 24-fold. Previously sulfate uptake, cysteine biosynthesis, and histidine biosynthesis genes were shown to be up-regulated and tryptophan biosynthesis genes were down-regulated in response to metabolite stress (Alsaker et al., 2010; Wang et al., 2013). The down-regulated biosynthesis of these amino acids in this study might account for the reduced biomass of DH2 strain (Figure 3). Sulfate uptake and cysteine biosynthesis genes were down-regulated 3- to 6-fold when cells were cultured under a high NADH availability condition by supplement of MV (Hönicke et al., 2012), which is in line with our result but contrary to a study showing highly up-regulated sulfate and cysteine biosynthesis

within cells under another high NADH availability condition: grown at neutral pH on glucose plus glycerol (Yoo et al., 2015). In addition, a total of forty 50S and 30S ribosomal proteins (L3-L6, L11-L36, S2, S3 and S10-S21) were up-regulated 2- to 3-fold in the DH2 strain. Also up-regulated were the proteins involved in thiamine metabolism CA_C2234 (2.2-fold), CA_C2971 (2.4-fold), CA_C2972 (6.4-fold), CA_C3112 (2.0-fold) and CA_P0106 (38.8-fold). Proteins involved in precorrin-2 biosynthesis (HemA, HemB, HemD and HemL) were up-regulated 3- to 5-fold, but the proteins CbiL, CbiC, CobP and CobT of the following processes for Vitamin B12 synthesis were down-regulated 4- to 9-fold. Several proteins LuxS, ParB, PabA, PlcA and CA_P0073 that are involved in quorum sensing were down-regulated 2.6, 10, 6.3, 7.5 and 2.3-fold, respectively, which should help the cells to reduce production of extracellular substances like biofilm.

3.7 Combined analysis of molecular basis under enhanced reducing power conditions

Currently, methods to effectively conserve reducing power in *C. acetobutylicum*, especially in genetic terms, are rather limited. More limited are the understandings of mechanisms enabling reducing power conservation. Supplement of electron carrier MV (Grupe and Gottschalk, 1992; Rao and Mutharasan, 1986) and chemostat culture at neutral pH on glucose plus glycerol (Girbal and Soucaille, 1994; Vasconcelos et al., 1994) have been shown to be able to enhance reducing power conservation in *C. acetobutylicum* over the years, and their molecular responses were recently studied

with transcriptomic (Hönicke et al., 2012) and quantitative transcriptomic-proteomic analyses (Yoo et al., 2015; Yoo et al., 2016), respectively. During the preparation of this manuscript, it was reported that a Δ*buk*Δ*ptb* mutant could also significantly enhance the reducing power in *C. acetobutylicum* under pH-controlled chemostat conditions, and a transcriptomic analysis was conducted to study the molecular basis (Yoo et al., 2017). Altogether, the MV addition, the chemostat culture at neutral pH on glycerol, the Δ*buk*Δ*ptb* mutation, and the NADH-compensation in this study represent the four most effective strategies at present for enhancing reducing power. Here, for the first time combined analysis of the molecular basis from these studies was performed, based on which potential mechanisms as well as some promising, yet understudied aspects of redox manipulation in *C. acetobutylicum* were concluded (Figure 5 and Table 5).

Generally, under the four different enhanced reducing power conditions cells showed some differences in gene/protein regulation, but they meanwhile shared important common regulation patterns, such as the dramatic down-regulation of acetone pathway and the switch of alcohol dehydrogenase from AdhE1 and BdhB to AdhE2 (Figure 5). In *Clostridium* hydrogenase is of particular interests as it has been considered responsible for the loss of reducing power. However, results of the four studies suggested that the regulation of redox partners flavodoxin and ferredoxin probably counted more in reducing power conservation. Future engineering of redox partners in *C. acetobutylicum* is a good way to demonstrate this. Furthermore, accumulating evidences showed that the C_4-metabolism in *C. acetobutylicum*

impacted on reducing power conservation considerably. For example, block of C_4 fluxes led to massive production of ethanol wherein loss of reducing power was calculated to be decreased significantly (Cooksley et al., 2012; Lehmann and Lütke-Eversloh, 2011; Lehmann et al., 2012b; Supplementary File 1, Table S3). So, *C. acetobutylicum* could be a yeast-like producer with nearly no reducing power lost (that is no H_2 produced), though mechanisms remain to be elucidated. Finally, it was speculated that NADH and NADPH might have different roles in reducing power conservation, and reducing power seemed to be better conserved via the form of NADH (Table 5). So far, the specific impact of NADPH on the central metabolism of *C. acetobutylicum* has been not elucidated and necessitates further research.

4. Discussion

Over the years, ineffective manipulations and inadequate understandings of the reducing power conservation in *C. acetobutylicum* have left us little to do with a most important problem regarding the substrate conversion: the cells lose large amounts of reducing power and produce considerable amounts of oxidation products like acetone, causing poor atom economies and low product yields. Here, by introducing an NADH-compensating module for the first time, an effective strategy for the conservation of reducing power is provided and valuable insights into the molecular basis are obtained.

4.1 “real” elimination of acetone under industrial conditions

Before this study, MV addition has been extensively employed to enhance the

reducing power in *C. acetobutylicum* (Grupe and Gottschalk, 1992; Jiang et al., 2009; Peguin et al., 1994; Rao and Mutharasan, 1986). Most recently, mutation of *ptb* and *buk* was also found to enhance the reducing power (Yoo et al., 2017). Although the MV addition and the Δ*buk*Δ*ptb* mutation moderately increased the total product yield, their effects seemed to be best during pH-controlled chemostat cultures which suffered from low product titers and were less favourable for industrialization (Grupe and Gottschalk, 1992; Yoo et al., 2017). During uncontrolled batch fermentation, the effects would be greatly offset (Hönicke et al., 2012; Jang et al., 2012; Peguin et al., 1994). Some researchers disrupted acetone formation genes (Jang et al., 2012; Jiang et al., 2009) or introduced an isopropanol dehydrogenase (Collas et al., 2012; Dai et al., 2012; Joungmin et al., 2012) to eliminate acetone. Nevertheless, these studies could not enhance the intracellular reducing power, and although acetone was not detected, "it" was actually accumulated at an equivalent amount of precursor acids or isopropanol. Consequently, the product yields were all apparently decreased (Table 6). Our study was different. By constructing an internal NADH-compensating module, the intracellular reducing power were effectively reinforced, thus acetone could be thoroughly abolished: no metabolites before or after the acetone pathways were accumulated, so the acetone pathway flux was eliminated in a real sense. At the same time, no butanol was sacrificed and the overall yield of alcohols was dramatically increased. This internal mechanism was also robust enough, so acetone could be effectively eliminated throughout the batch fermentations without pH-control and relatively high product titers could be obtained. Enhanced reducing power could

rescue metabolic intermediates from decarboxylation to lower molecular weight products and recover the process from low atom economies. Thus, the yield of total alcohols to glucose was drastically improved and reached 0.44 g/g, a yield much higher than those reported from previous studies (Table 6). Overall, this study presents the first strategy for efficient elimination of acetone under uncontrolled industrial conditions.

4.2 Valuable understandings on the conservation of reducing power

Previous studies aiming at manipulation of carbon conversion pathway genes failed to effectively eliminate acetone (Jang et al., 2012; Jiang et al., 2009; Kuit et al., 2012; Lütke-Eversloh and Bahl, 2011; Lehmann et al., 2012). Some researchers believed acetone formation has essential physiological roles in *C. acetobutylicum*, e.g., counteracting acidification and generating ATP (Desai et al., 1999a; Hartmanis et al., 1984). In this study, no solventogenic genes were manipulated and acetone could be efficiently eliminated with enhanced reducing power. This suggests that the intrinsic formation of acetone is actually a result of reducing power deficiency in *C. acetobutylicum*. In addition, while some researchers are trying manipulation of solventogenesis genes or hydrogenases to conserve the reducing power (Cooksley et al., 2012; Jang et al., 2014; Liu et al., 2015), this study suggests that the key to conservation of reducing power may not lie in these metabolic ends, but in the intermediate processes in central metabolism that are related to redox partners, C_4 metabolism, and possibly NADH and NADPH specificity. Therefore, this study provides novel understandings of the processes concerning reducing power

conservation and sets the direction of redox engineering of *C. acetobutylicum* in the future. The understandings should also be valuable for studying other solventogenic *Clostridium*, e.g., *Clostridium beijerinckii*, *Clostridium tyrobutyricum*, *Clostridium pasteurianum*, and *Clostridium thermocellum*. These solventogenic *Clostridium* strains have unique capabilities to biosynthesize a variety of fuels and bulk chemicals that are fundamentally important for humans from various low-cost renewable biomass resources. They have a lot in common with *C. acetobutylicum* with regard to the redox processes in central metabolism, and also suffer from the loss of intracellular reducing power (Biswas et al., 2015; Liu et al., 2016; Ma et al., 2015; Schwarz et al., 2017). The effective manipulation and understandings of reducing power conservation in this study will also help rational development of theses *Clostridium* species towards atom-economic production of a range of biofuels and alcohols.

4.3 Atom economy-based integration of bioprocesses

As a fuel and an important building block (Xu et al., 2014), 2,3-butanediol and its key downstream products were estimated to have a global market comparable to that of butanol (Köpke et al., 2014). Here, by integrating 2,3-butanediol production with butanol production, the redundant NADH that was typically wasted in 2,3-butanediol production (Bae et al., 2016; Kim et al., 2015), could be recruited to reduce the intermediates in butanol fermentation that would otherwise be decarboxylated to acetone with evolution of CO_2. As a result, the atom economy as well as the total

product value was able to be dramatically improved. This study presents a novel design of biobutanol process to improve its economics and should inspire more atom economy-based integration of bioprocesses to overall reduce the carbon footprint in fuels and bulk chemicals production.

5. Conclusions

A synthetic 2,3-butanediol biosynthesis pathway was systematically constructed in *C. acetobutylicum* as an NADH-compensating module, which could trigger effective conservation of intracellular reducing power. Enhanced reducing power recovered butanol from acetone-associated low economies. For the first time, acetone was thoroughly eliminated under uncontrolled industrial conditions, giving the highest solvent yield ever reported for butanol fermentation. Thus, it is the deficiency of reducing power rather than typically manipulated solventogenesis genes that essentially facilitates acetone formation. Molecular basis suggested that the mechanisms enabling reducing power conservation might lie in the intermediate processes in central metabolism. This study represents the first effective redox-based configuration of *C. acetobutylicum* that fundamentally upgraded the biobutanol process, and reveals more for further understanding and rational engineering of solventogenic *Clostridium*.

Acknowledgements

The authors thank Prof. Nigel P. Minton from the University of Nottingham for

kindly providing the ClosTron plasmids, and Prof. Sheng Yang from Shanghai Institutes for Biological Sciences for kindly providing pSY8 plasmid. This work was supported by the Jiangsu Provincial Natural Science Foundation of China (Grant No.: BK20150938); the National Nature Science Foundation of China (Grant No.: 21706123); the National Basic Research Program of China (973) (2013CB733602); the Major Research Plan of the National Natural Science Foundation of China (21390204); the key program of the National Natural Science Foundation of China (21636003); the Program for Changjiang Scholars and Innovative Research Team in University (IRT_14R28); the Priority Academic Program Development of Jiangsu Higher Education Institutions (PAPD), and the Jiangsu Synergetic Innovation Center for Advanced Bio-Manufacture.

References

Alsaker, K. V., Paredes, C., Papoutsakis, E. T., 2010. Metabolite stress and tolerance in the production of biofuels and chemicals: gene‐expression‐based systems analysis of butanol, butyrate, and acetate stresses in the anaerobe Clostridium acetobutylicum. Biotechnology and bioengineering. 105, 1131-1147.

Bae, S. J., Kim, S., Hahn, J. S., 2016. Efficient production of acetoin in Saccharomyces cerevisiae by disruption of 2,3-butanediol dehydrogenase and expression of NADH oxidase. Scientific Reports. 6, 27667.

Baer, S. H., Blaschek, H. P., Smith, T. L., 1987. Effect of Butanol Challenge and Temperature on Lipid Composition and Membrane Fluidity of Butanol-Tolerant Clostridium acetobutylicum. Applied & Environmental Microbiology. 53, 2854-61.

Biswas, R., Zheng, T., Olson, D. G., Lynd, L. R., Guss, A. M., 2015. Elimination of hydrogenase active site assembly blocks H2 production and increases ethanol yield in Clostridium thermocellum. Biotechnology for biofuels. 8, 20.

Collas, F., Kuit, W., Clément, B., Marchal, R., López-Contreras, A. M., Monot, F., 2012. Simultaneous production of isopropanol, butanol, ethanol and 2,3-butanediol by Clostridium acetobutylicum ATCC 824 engineered strains. AMB Express. 2, 45.

Cooksley, C. M., Zhang, Y., Wang, H., Redl, S., Winzer, K., Minton, N. P., 2012. Targeted mutagenesis of the Clostridium acetobutylicum acetone–butanol–ethanol fermentation pathway. Metabolic

Engineering. 14, 630.

Croux, C., Lee, J., Raynaud, C., Saint-Prix, F., Gonzalez-Pajuelo, M., Meynial-Salles, I., Soucaille, P., 2016. Construction of a restriction-less, marker-less mutant useful for functional genomic and metabolic engineering of the biofuel producer Clostridium acetobutylicum. Biotechnology for biofuels. 9, 23.

Dai, Z., Dong, H., Zhu, Y., Zhang, Y., Li, Y., Ma, Y., 2012. Introducing a single secondary alcohol dehydrogenase into butanol-tolerant Clostridium acetobutylicum Rh8 switches ABE fermentation to high level IBE fermentation. Biotechnology for biofuels. 5, 44.

Desai, R. P., Harris, L. M., Welker, N. E., Papoutsakis, E. T., 1999a. Metabolic Flux Analysis Elucidates the Importance of the Acid-Formation Pathways in Regulating Solvent Production by Clostridium acetobutylicum. Metabolic Engineering. 1, 206-213.

Desai, R. P., Nielsen, L. K., Papoutsakis, E. T., 1999b. Stoichiometric modeling of Clostridium acetobutylicum fermentations with non-linear constraints. Journal of biotechnology. 71, 191-205.

Girbal, L., Soucaille, P., 1994. Regulation of Clostridium acetobutylicum metabolism as revealed by mixed-substrate steady-state continuous cultures: role of NADH/NAD ratio and ATP pool. Journal of bacteriology. 176, 6433-6438.

Green, E. M., 2011. Fermentative production of butanol--the industrial perspective. Current opinion in biotechnology. 22, 337-43.

Grupe, H., Gottschalk, G., 1992. Physiological Events in Clostridium acetobutylicum during the Shift from Acidogenesis to Solventogenesis in Continuous Culture and Presentation of a Model for Shift Induction. Applied & Environmental Microbiology. 58, 3896-902.

Hönicke, D., Janssen, H., Grimmler, C., Ehrenreich, A., Lütke-Eversloh, T., 2012. Global transcriptional changes of Clostridium acetobutylicum cultures with increased butanol:acetone ratios. New Biotechnology. 29, 485-493.

Hartmanis, M. G. N., Klason, T., Gatenbeck, S., 1984. Uptake and activation of acetate and butyrate in Clostridium acetobutylicum. Applied Microbiology and Biotechnology. 20, 66-71.

Heap, J. T., Kuehne, S. A., Ehsaan, M., Cartman, S. T., Cooksley, C. M., Scott, J. C., Minton, N. P., 2010. The ClosTron: Mutagenesis in Clostridium refined and streamlined. Journal of Microbiological Methods. 80, 49-55.

Higashide, W., Li, Y., Yang, Y., Liao, J. C., 2011. Metabolic engineering of Clostridium cellulolyticum for production of isobutanol from cellulose. Applied & Environmental Microbiology. 77, 2727-33.

Jang, Y.-S., Im, J. A., Choi, S. Y., Im Lee, J., Lee, S. Y., 2014. Metabolic engineering of Clostridium acetobutylicum for butyric acid production with high butyric acid selectivity. Metabolic engineering. 23, 165-174.

Jang, Y., Lee, J., Lee, J., Park, J., Im, J., Eom, M., Lee, J., Lee, S., Song, H., Cho, J., Seung do, Y., Lee, S., 2012. Enhanced butanol production obtained by reinforcing the direct butanol-forming route in Clostridium acetobutylicum. Mbio. 3, 429-493.

Jiang, Y., Liu, J., Jiang, W., Yang, Y., Yang, S., 2014. Current status and prospects of industrial bio-production of n-butanol in China. Biotechnology Advances. 33, 1493-1501.

Jiang, Y., Xu, C., Dong, F., Yang, Y., Jiang, W., Yang, S., 2009. Disruption of the acetoacetate decarboxylase gene in solvent-producing Clostridium acetobutylicum increases the butanol ratio. Metabolic Engineering. 11, 284-291.

Jones, D. T., Woods, D. R., 1986. Acetone-butanol fermentation revisited. Microbiological Reviews. 50,

484.

Joungmin, L., Yusin, J., Sungjun, C., Jungae, I., Song, H. H., Junghee, C., Doyoung, S., Papoutsakis, E. T., Bennett, G. N., Sangyup, L., 2012. Metabolic engineering of Clostridium acetobutylicum ATCC 824 for isopropanol-butanol-ethanol fermentation. Applied & Environmental Microbiology. 78**,** 1416-1423.

Köpke, M., Gerth, M. L., Maddock, D. J., Mueller, A. P., Liew, F., Simpson, S. D., Patrick, W. M., 2014. Reconstruction of an acetogenic 2,3-butanediol pathway involving a novel NADPH-dependent primary-secondary alcohol dehydrogenase. Appl Environ Microbiol. 80**,** 3394-403.

Kim, J. W., Seo, S. O., Zhang, G. C., Jin, Y. S., Seo, J. H., 2015. Expression of Lactococcus lactis NADH oxidase increases 2,3-butanediol production in Pdc-deficient Saccharomyces cerevisiae. Bioresource Technology. 191**,** 512-519.

Kuit, W., Minton, N. P., López-Contreras, A. M., Eggink, G., 2012. Disruption of the acetate kinase (ack) gene of Clostridium acetobutylicum results in delayed acetate production. Applied Microbiology and Biotechnology. 94**,** 729-741.

Lütke-Eversloh, T., Bahl, H., 2011. Metabolic engineering of Clostridium acetobutylicum: recent advances to improve butanol production. Current opinion in biotechnology. 22**,** 634-47.

Lee, S., Kim, B., Park, K., Um, Y., Lee, J., 2012. Synthesis of pure meso-2, 3-butanediol from crude glycerol using an engineered metabolic pathway in Escherichia coli. Applied biochemistry and biotechnology. 166**,** 1801-1813.

Lehmann, D., Hönicke, D., Ehrenreich, A., Schmidt, M., Weuster-Botz, D., Bahl, H., Lütke-Eversloh, T., 2012. Modifying the product pattern of Clostridium acetobutylicum: physiological effects of disrupting the acetate and acetone formation pathways. Applied Microbiology and Biotechnology. 94**,** 743-754.

Li, H., Liao, J. C., 2014. A synthetic anhydrotetracycline-controllable gene expression system in Ralstonia eutropha H16. Acs Synthetic Biology. 4.

Li, L., Wang, Y., Li, K., Su, F., Ma, C., Xu, P., 2014a. Genome sequence of meso-2, 3-butanediol-producing strain Serratia marcescens ATCC 14041. Genome announcements. 2**,** e00590-14.

Li, Y. C., Xu, T., Tschaplinski, T. J., Engle, N. L., Yang, Y. F., Graham, D. E., He, Z. L., Zhou, J. Z., 2014b. Improvement of cellulose catabolism in Clostridium cellulolyticum by sporulation abolishment and carbon alleviation. Biotechnology for biofuels. 7**,** 25.

Liu, D., Chen, Y., Ding, F., Guo, T., Xie, J., Zhuang, W., Niu, H., Shi, X., Zhu, C., Ying, H., 2015. Simultaneous production of butanol and acetoin by metabolically engineered Clostridium acetobutylicum. Metabolic Engineering. 27**,** 107-114.

Liu, D., Chen, Y., Li, A., Ding, F., Zhou, T., He, Y., Li, B., Niu, H., Lin, X., Xie, J., 2013. Enhanced butanol production by modulation of electron flow in Clostridium acetobutylicum B3 immobilized by surface adsorption. Bioresource Technology. 129**,** 321-328.

Liu, J., Guo, T., Wang, D., Shen, X., Liu, D., Niu, H., Liang, L., Ying, H., 2016. Enhanced butanol production by increasing NADH and ATP levels in Clostridium beijerinckii NCIMB 8052 by insertional inactivation of Cbei_4110. Applied microbiology and biotechnology. 100**,** 4985-4996.

Ma, C., Ou, J., Xu, N., Fierst, J., Yang, S. T., Liu, X., 2015. Rebalancing Redox to Improve Biobutanol Production by Clostridium tyrobutyricum. Bioengineering. 3**,** 2.

Mermelstein, L. D., Papoutsakis, E. T., 1993. In vivo methylation in Escherichia coli by the Bacillus

subtilis phage phi 3T I methyltransferase to protect plasmids from restriction upon transformation of Clostridium acetobutylicum ATCC 824. Applied & Environmental Microbiology. 59**,** 1077-81.

Mermelstein, L. D., Welker, N. E., Bennett, G. N., Papoutsakis, E. T., 1992. Expression of Cloned Homologous Fermentative Genes in Clostridium Acetobutylicum ATCC 824. Biotechnology. 10**,** 190-195.

Oliver, J. W., Machado, I. M., Yoneda, H., Atsumi, S., 2013. Cyanobacterial conversion of carbon dioxide to 2, 3-butanediol. Proceedings of the National Academy of Sciences. 110**,** 1249-1254.

Peguin, S., Goma, G., Delorme, P., Soucaille, P., 1994. Metabolic flexibility of Clostridium acetobutylicum in response to methyl viologen addition. Applied Microbiology and Biotechnology. 42**,** 611-616.

Rao, G., Mutharasan, R., 1986. Alcohol production by Clostridium acetobutylicum induced by methyl viologen. Biotechnology Letters. 8**,** 893-896.

Schwarz, K. M., Grosse-Honebrink, A., Derecka, K., Rotta, C., Zhang, Y., Minton, N. P., 2017. Towards improved butanol production through targeted genetic modification of Clostridium pasteurianum. Metabolic engineering. 40**,** 124-137.

Shen, H. J., Cheng, B. Y., Zhang, Y. M., Tang, L., Li, Z., Bu, Y. F., Li, X. R., Tian, G. Q., Liu, J. Z., 2016. Dynamic control of the mevalonate pathway expression for improved zeaxanthin production in Escherichia coli and comparative proteome analysis. Metabolic Engineering. 38**,** 180-190.

Siemerink, M. A. J., Kuit, W., Contreras, A. M. L., Eggink, G., 2011. D-2,3-Butanediol Production Due to Heterologous Expression of an Acetoin Reductase in Clostridium acetobutylicum. Applied & Environmental Microbiology. 77**,** 2582-8.

Tracy, B. P., 2012. Improving butanol fermentation to enter the advanced biofuel market. MBio. 3**,** e00518-12.

Tummala, S. B., Junne, S. G., Papoutsakis, E. T., 2003a. Antisense RNA downregulation of coenzyme A transferase combined with alcohol-aldehyde dehydrogenase overexpression leads to predominantly alcohologenic Clostridium acetobutylicum fermentations. Journal of Bacteriology. 185**,** 3644.

Tummala, S. B., Welker, N. E., Papoutsakis, E. T., 2003b. Design of Antisense RNA Constructs for Downregulation of the Acetone Formation Pathway of Clostridium acetobutylicum. Journal of Bacteriology. 185**,** 1923.

Vasconcelos, I., Girbal, L., Soucaille, P., 1994. Regulation of carbon and electron flow in Clostridium acetobutylicum grown in chemostat culture at neutral pH on mixtures of glucose and glycerol. Journal of bacteriology. 176**,** 1443-1450.

Wang, Q., Venkataramanan, K. P., Huang, H., Papoutsakis, E. T., Wu, C. H., 2013. Transcription factors and genetic circuits orchestrating the complex, multilayered response of Clostridium acetobutylicum to butanol and butyrate stress. BMC systems biology. 7**,** 120.

Wang, S., Zhang, Y., Dong, H., Mao, S., Zhu, Y., Wang, R., Luan, G., Li, Y., 2011. Formic acid triggers the “acid crash” of acetone-butanol-ethanol fermentation by Clostridium acetobutylicum. Applied and environmental microbiology. 77**,** 1674-1680.

Wardwell, S. A., Yang, Y. T., Chang, H. Y., San, K. Y., Rudolph, F. B., Bennett, G. N., 2001. Expression of the Klebsiella pneumoniae CG21 acetoin reductase gene in Clostridium acetobutylicum ATCC 824. Journal of Industrial Microbiology & Biotechnology. 27**,** 220.

Xiao, Z., Lu, J. R., 2014. Strategies for enhancing fermentative production of acetoin: A review.

Biotechnology Advances. 32, 492.

Xie, N. Z., Li, J. X., Song, L. F., Hou, J. F., Guo, L., Du, Q. S., Yu, B., Huang, R. B., 2015. Genome sequence of type strain Paenibacillus polymyxa DSM 365, a highly efficient producer of optically active (R , R)-2,3-butanediol. Journal of Biotechnology. 195, 72-73.

Xu, Y., Chu, H., Gao, C., Tao, F., Zhou, Z., Li, K., Li, L., Ma, C., Xu, P., 2014. Systematic metabolic engineering of Escherichia coli for high-yield production of fuel bio-chemical 2,3-butanediol. Metabolic Engineering. 23, 22-33.

Xu, Y., Wang, A., Tao, F., Su, F., Tang, H., Ma, C., Xu, P., 2012. Genome sequence of Enterobacter cloacae subsp. dissolvens SDM, an efficient biomass-utilizing producer of platform chemical 2, 3-butanediol. Journal of bacteriology. 194, 897-898.

Xu, Z., Characterization of dehydrogenase mutants in continuous cultures of Clostridium acetobutylicum. München, Technische Universität München, Diss., 2014, 2014.

Yan, Y., Lee, C. C., Liao, J. C., 2009. Enantioselective synthesis of pure (R,R)-2,3-butanediol in Escherichia coli with stereospecific secondary alcohol dehydrogenases. Organic & Biomolecular Chemistry. 7, 3914-7.

Yoo, M., Bestelcorre, G., Croux, C., Riviere, A., Meynialsalles, I., Soucaille, P., 2015. A Quantitative System-Scale Characterization of the Metabolism of Clostridium acetobutylicum. Mbio. 6, e01808-15.

Yoo, M., Croux, C., Meynial-Salles, I., Soucaille, P., 2016. Elucidation of the roles of adhE1 and adhE2 in the primary metabolism of Clostridium acetobutylicum by combining in-frame gene deletion and a quantitative system-scale approach. Biotechnology for biofuels. 9, 92.

Yoo, M., Croux, C., Meynial-Salles, I., Soucaille, P., 2017. Metabolic flexibility of a butyrate pathway mutant of Clostridium acetobutylicum. Metabolic Engineering. 40, 138-147.

Figure 1 The rationale for NADH-compensation during butanol fermentation. In wild *C. acetobutylicum*, some intracellular reducing power is lost in H_2 form. In this case, considerable amounts of metabolic intermediates like AcAc-CoA are decarboxylated to acetone, possibly due to the deficiency of reducing power. By introducing a 2,3-butanediol synthesis pathway, extra NADH can be generated which may facilitate the conversion of intermediates into butanol instead of acetone.

Figure 2 Schematic diagram illustrating the systematic approach for construction of the NADH-compensating module based on 2,3-butanediol biosynthesis.

Figure 3 Comparison of metabolic flux distributions in the wild-type strain and the NADH-compensating strain DH2. Flux for glucose uptake was set to100 mole and the

other fluxes were determined as relative molar flux normalized to the flux for glucose uptake. Biomass is expressed as glucose equivalent. The absolute rate of glucose uptake ($r_{glucose}$) was calculated as the overall rate over the fermentation time. Cell growth rate was calculated as the overall specific growth rate (μ) before cells density start to decline. The negative values for acetate indicate that initial acetate in P2medium was used.

Figure 4 Major regulated pathways in the NADH-compensating DH2 strain revealed by proteomics analysis. Proteins or their gene locus (e.g., Cac3486) and reducing equivalents are shown only for regulated steps. Dash lines indicate no gene/protein is assigned at present. Red, blue and black arrows indicate up-regulated, down-regulated and non-regulated pathways, respectively.

Figure 5 Venn diagrams of regulated genes in central metabolic pathways under four enhanced reducing power conditions: Δ*buk*Δ*ptb* mutation (Yoo et al., 2017), MV addition (Hönicke et al., 2012), chemostat culture at neutral pH on glucose plus glycerol (Yoo et al., 2015) and NADH-compensation (this study). Genes are: *ack*, acetate kinase; *adc*, acetoacetate decarboxylase; *adhE1*, NADH-dependent aldehyde dehydrogenase; *adhE2*, NADH-dependent aldehyde-alcohol dehydrogenase; *bcd*, butyryl-CoA dehydrogenase; *bdhA*, *bdhB* and *bdhC*, NADPH-dependent butanol dehydrogenases; *buk*, butyrate kinase; CAP0059, alcohol dehydrogenase; *crt*, 3-hydroxybutyryl-CoA dehydratase; *ctfAB*, butyrate-acetoacetate COA-transferase; *etfAB*, electron transfer flavoprotein; *fcd*, FAD/FMN-containing butyryl-CoA dehydrogenase; *hbd*, 3-hydroxybutyryl-CoA dehydrogenase; *hydA*, hydrogenase; *ldh*,

lactate dehydrogenase; *pta*, phosphotransacetylase; *pdc*, pyruvate decarboxylase; *pfoAB*, pyruvate-ferredoxin/flavodoxin oxidoreductase. *ptb*, phosphate butyryltransferase; *thlA*, acetyl-CoA acetyltransferase.

Table 1 Bacterial strains and plasmids used in this study.

Plasmid or strain	**Relevant characteristics**	**Reference/Source**
pSY8	Expression plasmid, *ptb* promoter, Cm^R	(Jiang et al., 2009)
pMTL007C-E2	Gene disruption plasmid, *ltrA*, *Ll. ltrB* intron, pCB102, ColE1, Cm^R	(Heap et al., 2010)
pAN2	Methylation plasmid, *Φ3TI*, p15A *ori*, Tet^R	(Heap et al., 2010)
E. coli DH5a	Cloning strain	Laboratory stock
E. coli TOP10	Cloning strain	Invitrogen
C. acetobutylicum B3	CGMCC 5234, wild type	(Liu et al., 2013)
C. beijerinckii NCIMB 8052	ATCC 51743, type strain	American Type Culture Collection
B. subtilis 168	Type strain	Laboratory stock
Engineered *C. acetobutylicum* B3 strains:		
B3 Δ*alsR*	with disrupted *alsR* gene	This work
B3 (*alsR*)	overexpressing *alsR*	This work
B3 (*alsS*)	overexpressing *alsS*	This work
B3 ($alsS_{bsu}$)	overexpressing *alsS* from *B. subtilis*	This work
B3 (*alsD*)	overexpressing *alsD*	This work
B3 ($alsD_{bsu}$)	overexpressing *alsD* from *B. subtilis*	This work
B3 ($alsD_{bli}$)	overexpressing *alsD* from *B. licheniformis*	This work
B3 ($alsD_{ppo}$)	overexpressing *alsD* from *P. polymyxa*	This work
B3 ($alsD_{ecl}$)	overexpressing *alsD* from *E. cloacae*	This work
B3 ($alsD_{kpn}$)	overexpressing *alsD* from *K. pneumoniae*	This work
B3 ($alsD_{sma}$)	overexpressing *alsD* from *S. marcescens*	This work
B3($bdhA_{bsu}$)	overexpressing *bdhA* from *B. subtilis*	This work
B3($budC_{kpn}$)	overexpressing *budC* from *K. pneumoniae*	This work
B3(bdh_{cau})	overexpressing *bdh* from *C. autoethanogenum*	This work
B3(acr_{cbe})	Overexpressing *acr* from *C. beijerinckii*	This work
B3($alsD_{bsu}$-acr_{cbe})	Overexpressing *alsD* from *B. subtilis* and *acr* from *C. beijerinckii*	This work
B3($alsD_{bsu}$-$bdhA_{bsu}$)	Overexpressing both *alsD* and *bdhA* from *B. subtilis*	This work
B3($alsD_{bsu}$-RBS-acr_{cbe})	Overexpressing *alsD* from *B. subtilis* and *acr* from *C. beijerinckii* with RBS upstream of	This work

	acr	
B3(*alsD*$_{bsu}$-RBS-*bdhA*$_{bsu}$)	Overexpressing both *alsD* and *bdhA* from *B. subtilis* with RBS upstream of *bdhA*	This work
B3(*alsD*$_{bsu}$-RBS-*bdh*$_{cau}$)	Overexpressing *alsD* from *B. subtilis* and *bdh* from *C. autoethanogenum* with RBS upstream of *bdh*	This work
B3(*alsD*$_{bsu}$-RBS-*budC*$_{kpn}$)	Overexpressing both *alsD* and *budC* from *K. pneumonia* with RBS upstream of *budC*	This work
B3(*alsD*$_{bsu}$-RBS-*bdhA*$_{bsu}$-RBS-*alsS*$_{cac}$)	Overexpressing *alsD,bdhA* from *B. subtilis* and *alsS* from *C.acetobutylicum* with RBS	This work
B3(*alsD*$_{bsu}$-RBS-*bdhA*$_{bsu}$-RBS-*alsS*$_{bsu}$)	Overexpressing *alsD,bdhA,alsS* from *B. subtilis* with RBS	This work
B3(*alsD*$_{bsu}$-RBS-*bdhA*$_{bsu}$-RBS-*acr*$_{cbe}$)	Overexpressing *alsD,bdhA* from *B. subtilis* and *acr* from *C. beijerinckii* with RBS	This work

Table 2 Product patterns of *C. acetobutylicum* strains engineered for acetoin production.

Strain	Ethanol (g/L)	Butanol (g/L)	Acetone (g/L)	**Acetoin** (g/L)	Acids[a] (g/L)	Total solvent (g/L)	Solvent yield[b] (g/g)
B3 wild strain	**2.1**	**11.4**	**4.9**	**1.6**	**1.2**	**20.2**	**0.367**
B3 Δ*alsR*	1.9	10.7	4.4	1.4	1.1	18.4	-
B3 (*alsR*)	2.1	11.5	4.5	2.1	0.87	20.2	-
B3 (*alsS*)	1.5	9.1	3.0	1.7	1.2	15.3	-
B3 (*alsS*$_{bsu}$)	0.85	5.2	1.4	2.3	3.1	9.8	-
B3 (alsD)	1.8	11.8	2.2	5.0	0.83	20.8	0.372
B3 (*alsD*$_{bsu}$)	**1.9**	**12.0**	**1.9**	**6.1**	**0.71**	**21.9**	**0.418**
B3 (*alsD*$_{bli}$)	0.57	6.7	0.79	4.3	3.5	12.4	-
B3 (*alsD*$_{ppo}$)	1.1	9.9	1.2	3.6	1.9	15.8	-
B3 (*alsD*$_{kpn}$)	1.5	10.8	2.9	3.3	1.6	18.5	-
B3 (*alsD*$_{ecl}$)	1.8	11.6	3.2	4.0	1.3	20.6	-
B3 (*alsD*$_{sma}$)	1.5	11.0	3.2	4.1	1.8	19.8	-

[a]butyric and acetic acids.

[b]The solvent yield was calculated as the total solvent produced (g/L) divided by the glucose consumed (obtained by subtracting residual glucose from initial glucose, g/L). Initial glucose concentration was 60 g/L. Mass yields were determined only for strains with good performances.

Table 3 Product patterns of *C. acetobutylicum* strains engineered for 2,3-butanediol production.

Strain(construct)	Ethanol (g/L)	Butanol (g/L)	Acetone (g/L)	**Acetoin** (g/L)	2,3-BD (g/L)	Acids[a] (g/L)	Total solvent (g/L)	Solvent yield[b] (g/g)
B3 wild strain	**2.1**	**11.4**	**4.9**	**1.6**	**0.0**	**1.2**	**20.2**	**0.367**
B3(*bdhA*$_{bsu}$)	1.8	11.3	4.3	0.34	2.0	1.3	19.7	-
B3(*budC*$_{kpn}$)	2.2	12.1	4.7	0.47	3.3	0.59	22.8	0.390
B3(*bdh*$_{cau}$)	1.0	10.9	2.6	0.08	1.9	2.1	16.5	-
B3(*acr*$_{cbe}$)	1.7	10.8	3.5	0.01	1.5	1.6	17.5	-
B3(*alsD*$_{bsu}$-*acr*$_{cbe}$)	1.5	11.7	2.6	0.02	4.0	0.81	19.8	-
B3(*alsD*$_{bsu}$-*bdhA*$_{bsu}$)	1.8	11.7	2.1	1.3	4.2	1.0	21.1	-
B3(*alsD*$_{bsu}$-RBS-*acr*$_{cbe}$)	1.9	11.5	1.4	0.01	5.0	1.4	19.8	-
B3(*alsD*$_{bsu}$-RBS-*bdhA*$_{bsu}$)	**1.9**	**12.1**	**2.2**	**0.9**	**7.9**	**0.65**	**25.0**	**0.416**
B3(*alsD*$_{bsu}$-RBS-*bdh*$_{cau}$)	1.8	12.8	2.1	0.02	4.3	0.99	21	-
B3 (*alsD*$_{bsu}$-RBS-*budC*$_{kpn}$)[c]	0.3	10.3	3.6	0.03	0.11	1.2	14.3	-
B3(*alsD*$_{bsu}$-RBS-*bdhA*$_{bsu}$ -RBS-*alsS*$_{cac}$)	1.0	9.2	2.9	1.2	2.6	2.5	16.9	-
B3(*alsD*$_{bsu}$-RBS-*bdhA*$_{bsu}$ -RBS-*alsS*$_{bsu}$)	1.0	8.9	2.7	0.93	4.6	1.7	18.1	-
B3(*alsD*$_{bsu}$-RBS-*bdhA*$_{bsu}$ -RBS-*acr*$_{cbe}$)[d]	**3.2**	**12.1**	**0.29**	**0.01**	**7.2**	**1.1**	**22.8**	**0.439**

[a]butyric and acetic acids.

[b]The solvent yield was calculated as the total solvent produced (g/L) divided by the glucose consumed (obtained by subtracting residual glucose from initial glucose, g/L). Mass yields were determined only for strains with good performances.

[c]Despite repeated attempts, something abnormal happened: no 2,3-butanediol was obtained in this case and both acetoin and ethanol were disappeared.

[d]The final strain, designated DH2.

Table 4 Differentially expressed proteins in central metabolic processes in the NADH-compensating strain DH2.

Locus	Gene	FC[a] (acidogenic)	FC[a] (solventogenic)	Protein function
Glycolysis				
CA_C0518	*pyk*	3.6	3.6	Pyruvate kinase
Pyruvate node				
CA_C3552	*ldh2*	3.2	2.6	L-lactate dehydrogenase 2
CA_C2229	*pfoA*	0.9	0.3	Pyruvate-ferredoxin/flavodoxin oxidoreductase
CA_C2499	*pfoB*	0.9	0.0	Pyruvate-ferredoxin/flavodoxin oxidoreductase
CA_P0025	*pdc*	0.0	0.03	Pyruvate decarboxylase
CA_C0980	*pfl*	1.1	0.5	Pyruvate-formate lyase
CA_C2458		1.5	0.4	2-oxoacid:ferredoxin oxidoreductase
CA_C2459		1.4	0.4	2-oxoacid:ferredoxin oxidoreductase
Acetone formation				
CA_P0163	*ctfA*	0.0009	0.03	Butyrate-acetoacetate CoA-transferase subunit A
CA_P0164	*ctfB*	0.003	0.03	Butyrate-acetoacetate CoA-transferase subunit B
CA_P0165	*adc*	0.3	0.2	Acetoacetate decarboxylase
butyryl-CoA synthesis				
CA_C2542	*fcd*	11.5	8.3	FAD/FMN-containing dehydrogenase
CA_C2543	*etfA*	43.6	42.4	Electron-transferring flavoprotein large subunit
CA_C2544	*etfB*	22.9	52.2	Electron-transferring flavoprotein small subunit
Aldehyde/alcohol dehydrogenase and redox partners				
CA_C3298	*bdhB*	0.4	0.2	NADPH-dependent butanol dehydrogenase
CA_C3392	*bdhC*	0.9	0.4	NADPH-dependent butanol dehydrogenase
CA_P0059		0.3	0.4	Alcohol dehydrogenase
CA_P0162	*adhE1*	0.02	0.03	NADH-dependent aldehyde dehydrogenase
CA_P0035	*adhE2*	3.4	21.0	Bifunctional NADH-dependent aldehyde-alcohol dehydrogenase
CA_C0303		0.4	0.4	Ferredoxin
CA_C3486		3.2	7.3	Multimeric flavodoxin

[a]FC, Fold Change; Only proteins with FC ≥ 2 or FC ≤ 0.5 were considered as differentially expressed protein.

Table 5 Main conclusions concerning the molecular basis of reducing power conservation *in C. acetobutylicum*.

Conclusions	Major evidences/references

AdhE2 rather than AdhE1 or BdhB is preferred under high reducing power conditions	●AdhE1 and BdhB are typically used for solvent production, but they were replaced with AdhE2 under all four enhanced reducing power conditions (Hönicke et al., 2012; Yoo et al., 2015; Yoo et al., 2017; this study)
Flavodoxin (CA_C3486) may account more for reducing power conservation than hydrogenase and its key partner ferredoxin (CA_C0303)	●no hydrogenase was down-regulated under all four enhanced reducing power conditions (Hönicke et al., 2012; Yoo et al., 2015; Yoo et al., 2017; this study) ●repression or disruption of *hydA* had little impact on products (Cai et al., 2013; Jang et al., 2014) ●up-regulation of CA_C3486 and/or down-regulation of CA_C0303 was observed under all four enhanced reducing power conditions (Hönicke et al., 2012; Yoo et al., 2015; Yoo et al., 2017; this study) ●flavodoxin (CA_C3486) was suggested to be a better substrate for ferredoxin/flavodoxin-NAD+ reductase than for hydrogenase (Yoo et al., 2015)
The C_4-metabolism in *C. acetobutylicum* exerts important influences on reducing power conservation	●Δ*buk*Δ*ptb* mutation dramatically enhanced reducing power supply (Yoo et al., 2017) ●butyryl-CoA dehydrogenase complex (either EtfAB-Bcd or EtfAB-Fcd) was significantly up-regulated under all four enhanced reducing power conditions (Hönicke et al., 2012; Yoo et al., 2015; Yoo et al., 2017; this study) ●block of C_4-product fluxes made the cells a yeast-like ethanol producer with less H_2 evolution (Cooksley et al., 2012; Lehmann and Lütke-Eversloh, 2011; Lehmann et al., 2012b; this study)
Reducing power might be better conserved via the form of NADH than via NADPH.	●electron flux through NADH was dramatically increased whereas the flux through NADPH was dramatically decreased under enhanced reducing power conditions (Yoo et al., 2015;Yoo et al., 2017) ●NADPH-dependent BdhB was replaced with NADH-dependent AdhE2 under all four enhanced reducing power conditions (Hönicke et al., 2012; Yoo et al., 2015; Yoo et al., 2017; this study)

Table 6 Comparison of the best results regarding elimination of acetone in *C. acetobutylicum* obtained with different strategies.

Strategy	Acetone (g/L)	Total solvent (g/L)	Solvent yield (g/g glucose)	Reference
Reference wild strains	6.0	20.0	0.350	(Green, 2011)

MV addition, pH = 4.5	2.0	16.7	0.355	(Peguin et al., 1994)
Disruption of *buk* and *pta*, and overexpression of a mutant *adhE1*	1.5	21.4	0.331	(Jang et al., 2012)
Disruption of *buk* and *ptb*, chemostat culture, pH = 4.4	0.46	10.4	0.361	(Yoo et al., 2017)
Disruption of *adc*, supplemented with $CaCO_3$ and MV	0.10	16.5	0.330	(Jiang et al., 2009)
Conversion of acetone to isopropanol by a secondary alcohol dehydrogenase	0	23.88	0.314	(Dai et al., 2012)
Construction of an NADH-compensating module	**0.29**	**22.8**	**0.439**	**This study**

Highlights:

- An NADH-compensating module was constructed in *Clostridium acetobutylicum*.
- The module triggered apparent conservation of intracellular reducing power.
- Acetone was efficiently eliminated, giving the highest solvent yield ever reported.
- Reducing power rather than solventogenesis genes dominate acetone formation.
- Molecular basis involved redox partners, C4-metabolism and cofactor specificity.

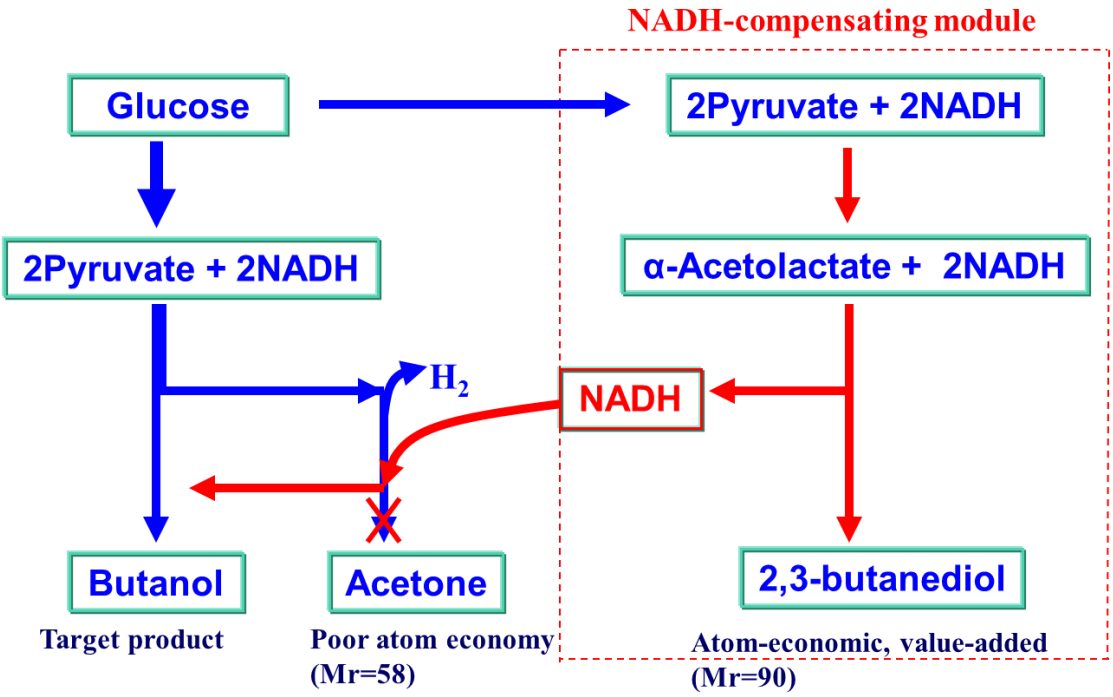

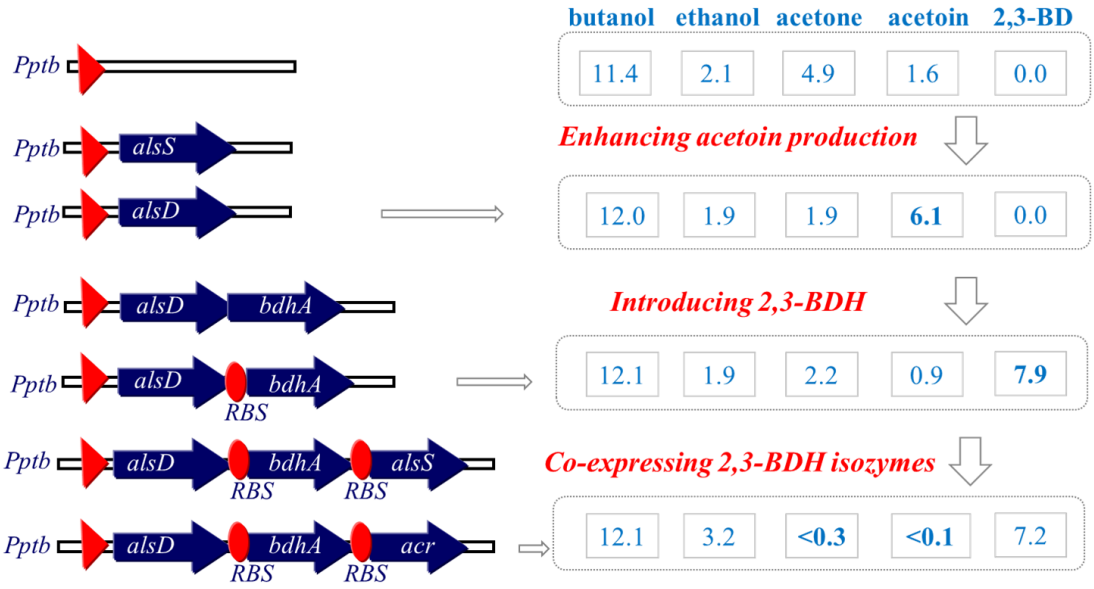

W: wild strain

$r_{glucose}$ = -0.0083 mol/gDCW/h

μ = 0.070/h

D: engineered strain DH2

$r_{glucose}$ = -0.0066 mol/gDCW/h

μ =0.038/h

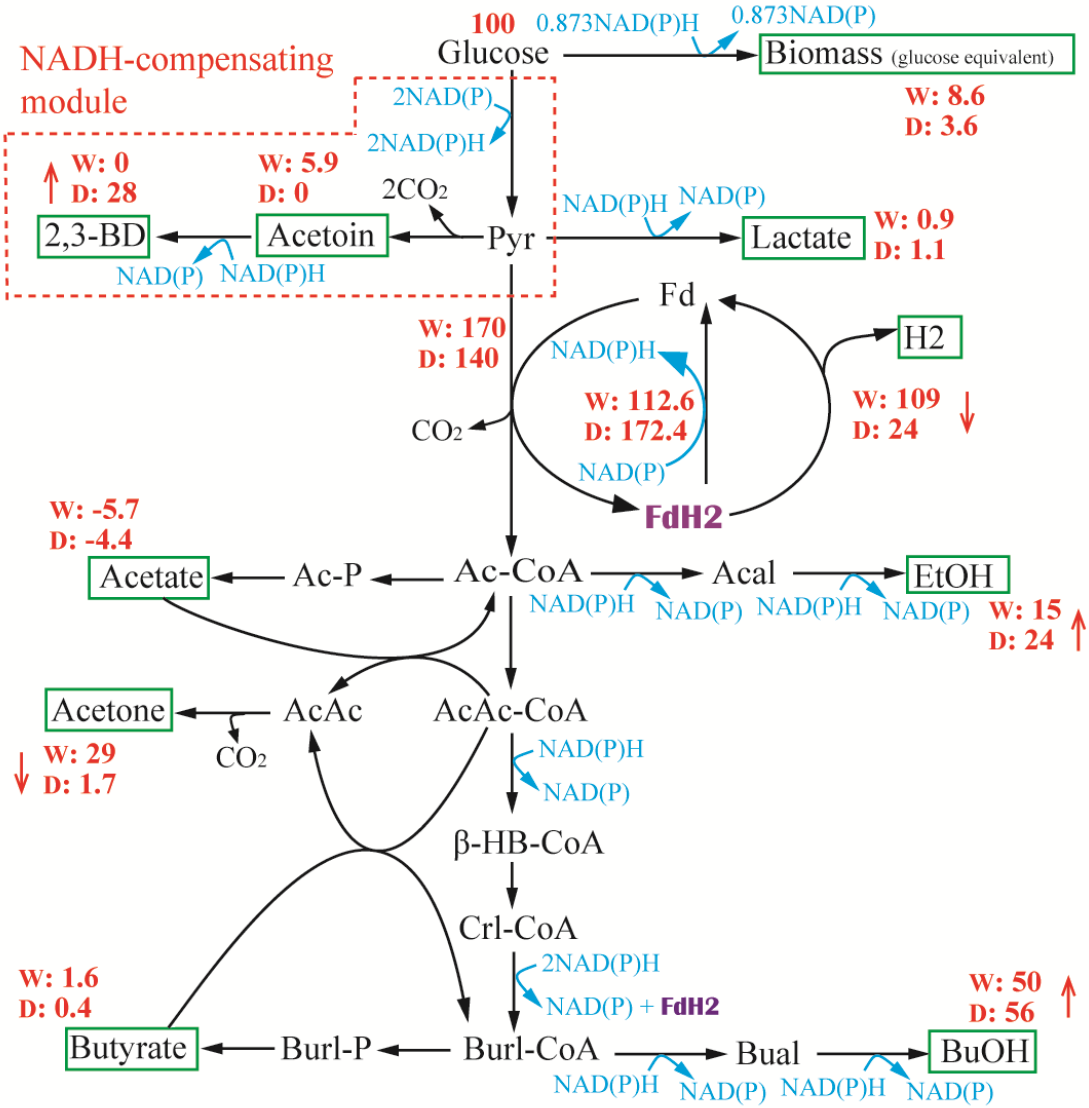

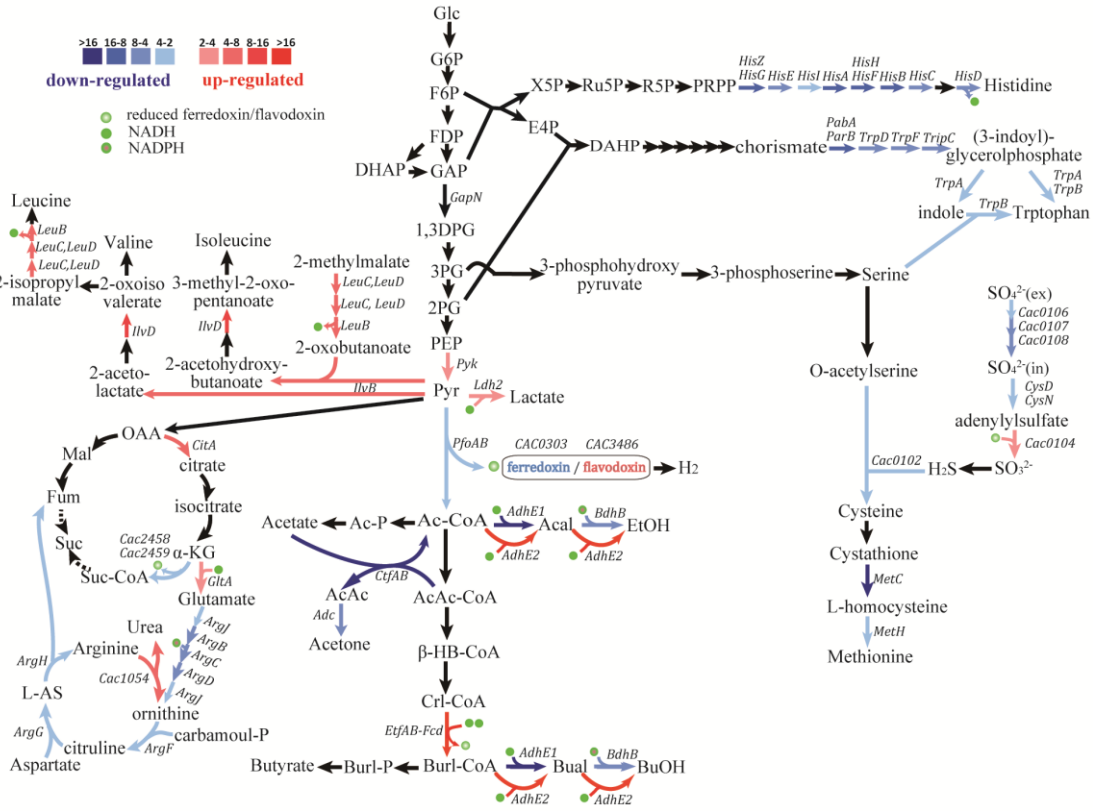
>16 16-8 8-4 4-2
down-regulated
2-4 4-8 8-16 >16
up-regulated
reduced ferredoxin/flavodoxin
NADH
NADPH
Glc
G6P
F6P
FDP
DHAP
GAP
1,3DPG
3PG
2PG
PEP
Pyr
Lactate
X5P
Ru5P
R5P
PRPP
Histidine
E4P
DAHP
chorismate
(3-indoyl)-glycerolphosphate
indole
Trptophan
3-phosphohydroxy pyruvate
3-phosphoserine
Serine
O-acetylserine
Cysteine
Cystathione
L-homocysteine
Methionine
Leucine
Valine
Isoleucine
2-isopropyl malate
2-oxoiso valerate
3-methyl-2-oxo-pentanoate
2-methylmalate
2-oxobutanoate
2-aceto-lactate
2-acetohydroxy-butanoate
OAA
Mal
Fum
Suc
Suc-CoA
citrate
isocitrate
α-KG
Glutamate
Urea
Arginine
ornithine
L-AS
citruline
carbamoul-P
Aspartate
Acetate
Ac-P
Ac-CoA
Acal
EtOH
AcAc
AcAc-CoA
Acetone
β-HB-CoA
Crl-CoA
Burl-P
Burl-CoA
Bual
BuOH
Butyrate
ferredoxin / flavodoxin
H2
SO4 2-(ex)
SO4 2-(in)
adenylylsulfate
H2S
SO3 2-

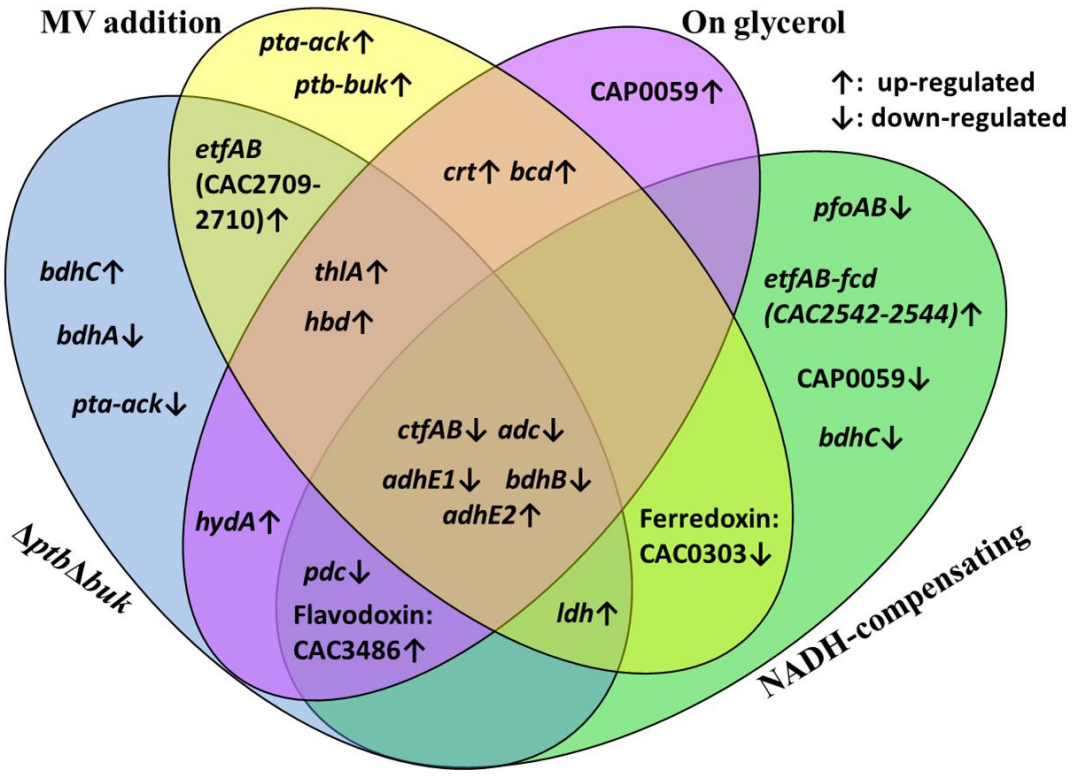
MV addition
On glycerol
↑: up-regulated
↓: down-regulated
pta-ack↑
ptb-buk↑
CAP0059↑
etfAB (CAC2709-2710)↑
crt↑ bcd↑
pfoAB↓
bdhC↑
thlA↑
hbd↑
etfAB-fcd (CAC2542-2544)↑
bdhA↓
CAP0059↓
pta-ack↓
bdhC↓
ctfAB↓ adc↓
adhE1↓ bdhB↓
adhE2↑
hydA↑
Ferredoxin: CAC0303↓
pdc↓
Flavodoxin: CAC3486↑
ldh↑
ΔptbΔbuk
NADH-compensating